Estimating Mixed Layer Height from Cloud-Aerosol Backscattering with Doppler Lidar

NAME:

Muhammad Akmal Hakim Rozliaiani 16362588

DATE:

October 2023

Abstract

Remote sensing techniques are frequently employed to ascertain the mixed layer height (MLH), a crucial parameter for assessing air quality. The mixed layer is situated within the planetary boundary layer, where particle concentrations, such as aerosols, are at their highest compared to the free atmosphere. Leveraging the capacity to measure the vertical atmospheric profile, remote sensing instruments like Doppler lidar can assess the attenuated backscatter of particles, providing vital data for MLH computation. During this study, a Halo Photonics Streamline Doppler Lidar was deployed for a 3-week period at Kaitorete Spit to capture vertical stare measurements of the atmosphere. The data underwent filtering using the threshold method to remove unwanted attenuated backscatter data, while the gradient or derivative method was applied to the backscatter data to determine the MLH. It was observed that the MLH tends to be larger during the daytime, gradually expanding from sunrise to evening. Conversely, at night, the MLH showed a gradual decrease on certain days.

1) Introduction

The investigation of the atmospheric boundary layer (ABL), also referred to as the planetary boundary layer (PBL), has played a pivotal role in enhancing our understanding of atmospheric dynamics in the lowest part of the atmosphere. Within the planetary boundary layer, there exists a region known as the mixing layer. This layer facilitates the mixing of particles originating from the surface and the lower atmosphere. Gaseous and particulate emissions from the Earth's surface are effectively dispersed and mixed within this layer, primarily due to the turbulent processes that occur within it (Schween, Hirsiko, Löhnert, & Crewell, 2014). The turbulence within the mixing layer plays a crucial role in transporting various atmospheric particles, including gases, moisture, aerosols, and pollutants, from the Earth's surface to the upper atmosphere.

Hence, the Mixing Layer Height (MLH) stands out as a vital parameter with significant implications for applications in the assessment of air quality (Schween, Hirsiko, Löhnert, & Crewell, 2014). MLH serves as an essential factor influencing near-surface air quality parameters, as it governs the volume over which emitted pollutants disperse (Wang & Wang, 2014). Given the rise in economic development and its associated increase in pollution, particularly in developing countries, understanding MLH becomes pivotal for both the environmental science community and the public (Wang & Wang, 2014). Additionally, MLH has implications for the rate of warming driven by the heightened presence of greenhouse gases (Wang & Wang, 2014).

Several factors can induce turbulence within the mixing layer, including the heating of the air near the Earth's surface. This heating leads to the development of temperature and pressure gradients within the air, and it is also influenced by wind shear. During daylight hours, the turbulent mixing in the atmospheric boundary layer is primarily driven by solar radiation energy. Most of this energy is absorbed by the Earth's surface and is subsequently re-emitted into the atmosphere as long-wave terrestrial radiation and the turbulence is generated by heat fluxes (Schween, Hirsiko, Löhnert, & Crewell, 2014). The amount of incoming solar radiation also was influence by the formation of clouds on the atmosphere and thus cause the turbulent heat fluxes from the surface into the atmosphere.

At night, the land surface cools more rapidly than the overlying atmosphere due to the higher emission of long-wave radiation (Wang & Wang, 2014). This results in an increase in temperature with height above the surface, creating a temperature inversion. This inversion gives rise to the development of a stable nocturnal boundary layer (NBL) near the surface, situated below the residual layer (RL) (Wang & Wang, 2014).

To ascertain the mixed layer height, a range of technical instruments is widely employed for turbulent parameter estimation in the atmospheric boundary layer and for determining the mixing layer height. These tools include Doppler sodars, radio acoustic systems, and Doppler lidars, which are well-suited for the task as they provide real-time meteorological data with the necessary spatial and temporal resolution (Banakh, Smalikho, & Falits, 2021). Another commonly used instrument for determining the mixed layer height is the radiosonde, which can measure various parameters like temperature, humidity, or Richardson number (Schween, Hirsiko, Löhnert, & Crewell, 2014). There are four widely accepted methods based on individual atmospheric variables: the potential temperature (θ) profile, the minimum vertical gradient of relative humidity (RH), specific humidity (q), and atmospheric refractivity (N) (Wang & Wang, 2014). To address the limitations of radiosonde measurements in terms of temporal resolution, remote sensing techniques like Doppler lidar can be implemented (Beamesderfer, et al., 2023).

Lidar (Light Detection and Ranging) is a technology that has been employed for studying atmospheric science since the early to mid-20th century. Lidar's capability lies in determining the backscatter coefficient of particles, such as aerosols, based on factors like concentration, size, and optical properties of these particles (Schween, Hirsiko, Löhnert, & Crewell, 2014). Assuming that aerosols primarily originate from the Earth's surface, turbulent mixing results in a relatively uniform high concentration of aerosols within the Mixing Layer (ML), with a gradual decrease in concentration as altitude increases (Schween, Hirsiko, Löhnert, & Crewell, 2014). Consequently, it becomes feasible to derive the Mixing Layer Height (MLH) from lidar-based measurements of the backscatter coefficient.

Doppler lidar has emerged as a widely adopted instrument in recent years, particularly with the commercialization of low-cost Doppler lidar technology, which has significantly accelerated atmospheric research. This remote sensing method harnesses the Doppler effect. When a pulse is emitted into the atmosphere, the laser light propagates at the speed of light, scatters off particles, and the resulting backscatter is measured by the Doppler lidar (Manninen, 2019). When pointed vertically, Doppler lidar can directly measure vertical velocity with exceptional vertical and temporal resolution, making it a valuable tool for boundary layer investigations (Manninen, 2019). The vertical velocity data from the vertical profile measurements can also be used to derive the mixed layer height. Dewani et al. (2023) proposed a method for estimating the mixed layer height by applying variance analysis to the vertical velocity data obtained from Doppler lidar.

The backscatter coefficient measured by Doppler lidar can also be utilized to determine the mixed layer height. There are five effective methods for estimating the mixing layer height: the threshold method, gradient or derivative method, idealized gradient method, wavelet method, and variance method (Emeis, Schafer, & Munkel, 2008). The threshold method is frequently mentioned in the literature for data quality control. Dewani et al. (2023) employed a signal-to-noise ratio (SNR) for Doppler lidar data quality control, setting a backscatter intensity (SNR+1) threshold at 1.005. While the choice of the threshold may seem arbitrary, conducting an investigation over a sufficiently long dataset can usually yield a value that provides satisfactory results in most cases (Manninen, 2019). The gradient or derivative method stands out as one of the most effective approaches for estimating the mixing layer height, as it can provide a numerical estimate of the mixing layer's approximate height (Emeis, Schafer, & Munkel, 2008).

The objective of this paper is to determine the mixing layer height (MLH) from Doppler lidar measurements of cloud and aerosol backscatter and to explore potential variations in MLH thickness over time. We will utilize the threshold and gradient methods, as suggested by Emeis et al. (2008), to estimate the mixing layer height. Broadly, existing studies concur that MLH is most reliably retrieved from aerosol backscatter data during the noon hour. This implies that the mixing layer tends to reach its maximum thickness around this time and thins out during the night. Aerosol were observed mostly confined below 1km altitude using lidar instrument (Dey & Tripathi, 2014). This means that the high aerosol concentration should be observed inside the mixing layer height.

2) Data Acquisition and Instrument

This analysis is based on observations conducted at Kaitorete Spit, a site owned by Tāwhaki. Kaitorete Spit is a geographical feature situated on the eastern coast of New Zealand's South Island, specifically in the Canterbury region, approximately 75 km southwest of Christchurch. Tāwhaki has historically utilized this site for research and development (R&D) within the aerospace industry, as well as for the conservation and rejuvenation of unique species (Ministry of Business, Inovation and Employment, 2022). A Doppler lidar instrument was set up and deployed on the site, as depicted in Figure 1(a, during a three-week period, from September 6th, 2023, to September 29th, 2023. Throughout this deployment, we encountered several technical challenges, one of which was a power outage. As a result of this event, the data obtained was limited to just one week's worth, spanning from September 6th to 7th and from September 14th to 18th, 2023. On September 29th, 2023, a weather balloon was launched at the site with the purpose of examining the Atmospheric Boundary Layer (ABL) using radiosonde data and comparing it to the boundary layer data obtained from the Doppler lidar.

(a) (b)

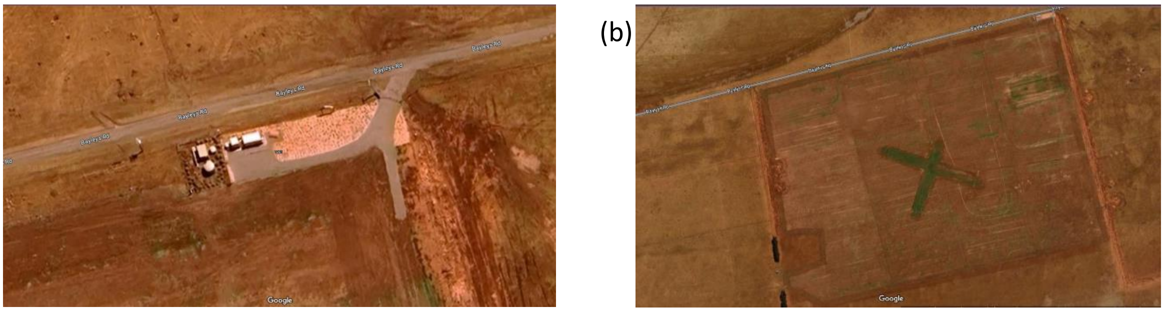

Figure 1. (a) We placed the Doppler lidar at the Tāwhaki site to capture readings. (b) The 'X' marks the location where the weather balloon was launched.

2.1) Doppler Lidar

The instrument utilized in this study is a Doppler lidar developed by Halo, specifically the Halo Photonics Streamline XR. This Doppler lidar is a pulsed Doppler lidar system that employs heterodyne detection and a fibre-optic system(Manninen, 2019). his lidar is considered eye-safe, as it operates at a wavelength of 532nm, enabling it to achieve a high pulse repetition rate. Depending on the environmental conditions, the lidar can measure data up to a range of 10km and possesses full hemispherical scanning capabilities (Manninen, 2019). The Streamline XR Doppler lidar is capable of performing three types of scanning patterns: vertical stare scan, conical scan (known as VAD or Vertical Azimuth Display), and RHI (Range Height Indicator) sweep scan.

During the Doppler lidar deployment, we employed all scanning types with specific targeting of data. However, for the purpose of this paper, we exclusively utilized the vertical stare scan to obtain the vertical profile of the atmosphere. The vertical stare scan mode enabled the Doppler lidar to measure parameters such as attenuated backscatter ($m^{-1}\,s^{-1}$) denoted as β, intensity (SNR+1) and doppler velocity (ms^{-1}) which, in this scanning pattern, represents the vertical velocity.

2.2) Weather Balloon

The balloon employed for this project was of the latex type, with a 1m diameter when inflated. Helium gas was used to inflate the balloon, and this process was conducted with the use of gloves to prevent direct contact, which could otherwise contaminate the latex and affect overall performance. The balloon had an approximate flight time of 40 minutes and was equipped with a radiosonde capable of measuring various atmospheric parameters, including altitude, temperature, humidity, and air pressure. Data obtained from the radiosonde proved to be a valuable method for estimating the Atmospheric Boundary Layer (ABL) based on the measured atmospheric parameters.

3) Method

The data collected from the Doppler lidar will undergo further analysis, involving techniques for quality control. In this section, we will delve into the methods used to filter and estimate the mixed layer height (MLH) from the Doppler lidar data. We will employ a threshold method, which utilizes the Signal-to-Noise Ratio (SNR) and vertical velocity to filter the data. Additionally, we will discuss a method developed by S. Emeis et al. (2008) that employs gradient or derivative techniques for estimating the MLH. Both of these methods have been implemented using Python code, and the code can be found in the Appendices section.

3.1) Vertical Stare Data

As previously mentioned in Section 3.1, we will obtain attenuated backscatter, intensity (SNR+1), or SNR (intensity-1), and vertical velocity from the Doppler lidar. The Signal-to-Noise Ratio (SNR) measures the strength of the return signal after it interacts with particles in the atmosphere (Newsom & Krishnamurthy, 2022). To visualize the data, we created time-height plots for all measurements acquired by the Doppler lidar between September 14th and 18th, 2023. During this period, the lidar collected data continuously for a full 24 hours each day. It's worth noting that the Doppler lidar time was recorded in decimal hours and the UTC time zone, which is 11 hours ahead of New Zealand local time. For instance, sunrise in New Zealand at 0700 hours corresponds to 1800 hours in UTC time.

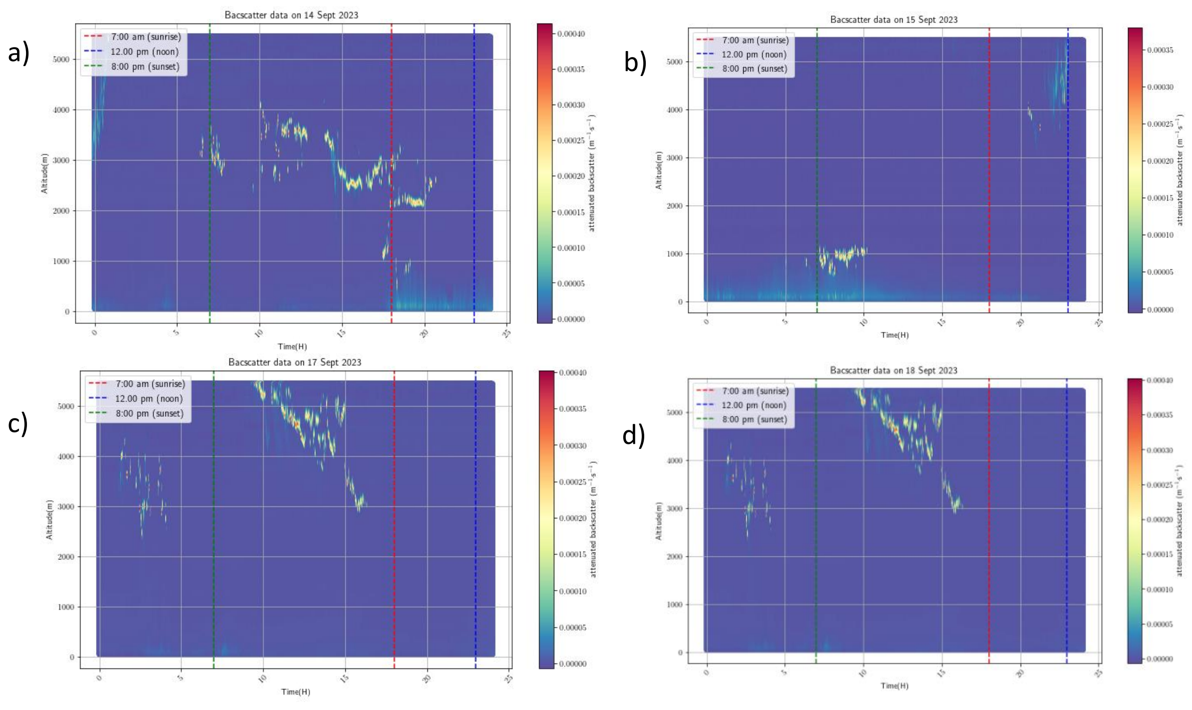

Figure 2. The time altitude plot for the attenuated backscatter raw data. (a), (b), (c) and (d) represent the plot at different day.

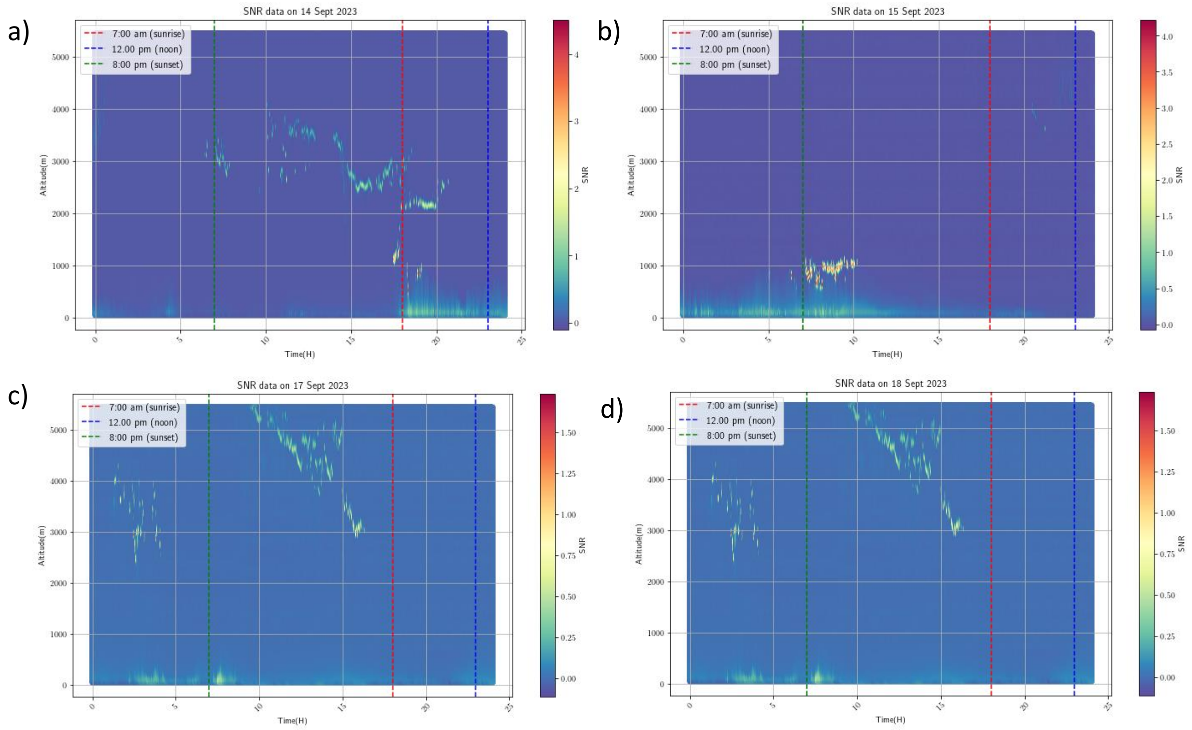

Figure 3. The time altitude plot for the SNR raw data. (a), (b), (c) and (d) represent the plot at different day.

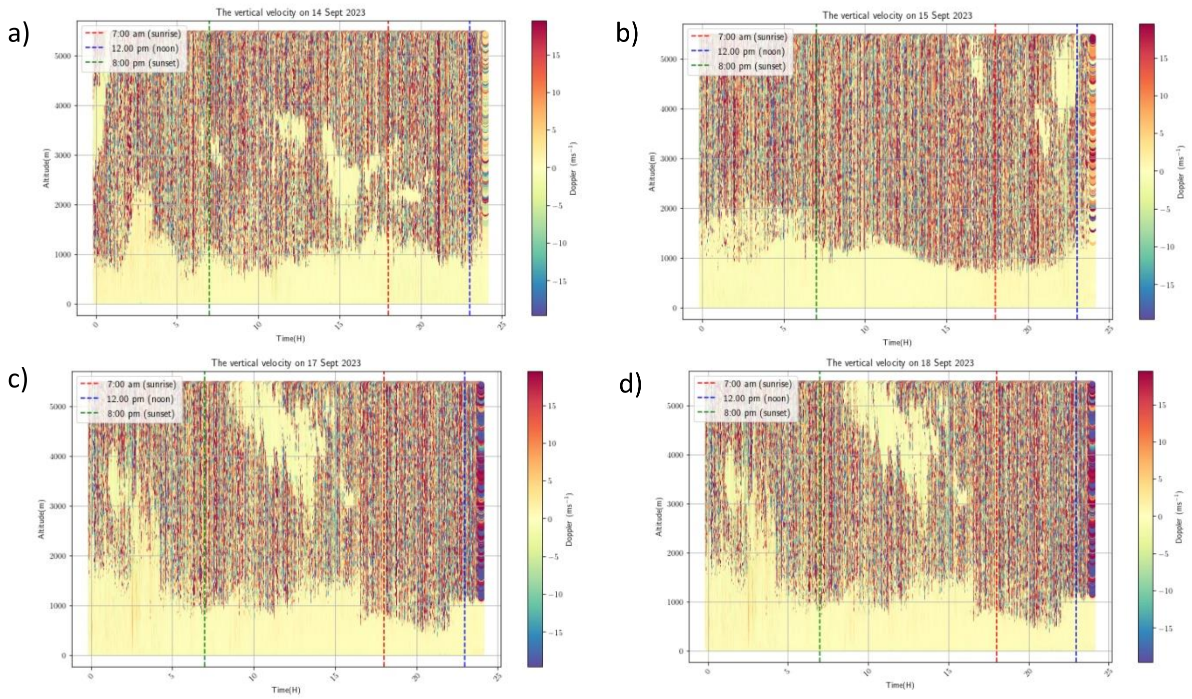

Figure 4. The time altitude plot for the vertical velocity raw data. (a), (b), (c) and (d) represent the plot at different day.

The data plots in both Figure 2 and Figure 3 exhibit striking similarities, as both measurements capture observations of light backscatter from clouds and aerosols. There are regions in the plot where measurements are notably higher than in other areas. For example, in Figure 2(a), we observe high backscatter coefficient readings at mid-latitudes, between 2000m and 4000m. This suggests a higher concentration of scattering or reflection in that region, likely due to an increased concentration of particles. We also notice a subtle but significant backscatter at lower altitudes, particularly in Figure 2(b) and Figure 3(b). The structure of the planetary boundary layer is not evident from the attenuated backscatter and SNR raw data plots, necessitating further analysis. However, we can tentatively discern the structure of the planetary boundary layer in Figure 3, particularly around lower altitudes in the atmosphere, where most of the vertical velocity falls within the range of $\pm 5ms^{-1}$.

3.2) Threshold method

This method has been widely employed in numerous papers to filter data from Doppler lidar by establishing a minimum SNR threshold. Applying this method eliminates poor-quality data while retaining good data. The minimum threshold value was determined using an approach outlined by N. Dewani et al. (2023), where the threshold was determined by identifying the SNR value at which the occurrence of vertical velocities between $\pm 5ms^{-1}$ is higher compared to other vertical velocities.

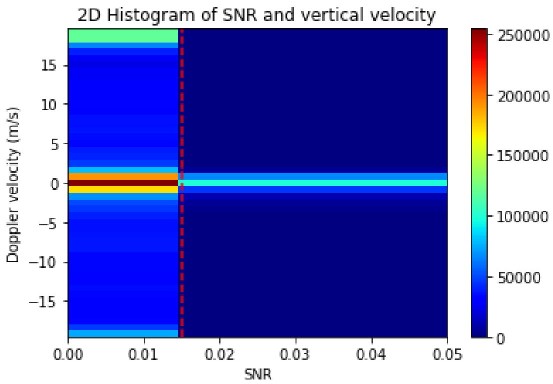

Figure 5. A 2D histogram of SNR and vertical velocity. The dashed red line indicates the SNR threshold of 0.015

The occurrence of data within the range of ±19 m/s is higher before reaching the threshold value, as evident in the 2D histogram shown in Figure 5. By selecting data with SNR values greater than the threshold, we expect the data to be concentrated around the planetary boundary layer, building upon our initial observations in Figure 4. The attenuated backscatter data will be filtered using a threshold of 0.015. We will also apply a logarithmic transformation to the filtered attenuated backscatter data to facilitate visualization. This approach aligns with the method used by Newsom and Krishnamurthy (2022) to improve data visualization.

3.3) Gradient or Derivative Methods

This method was initially proposed by Hayden et al. (1997) and Flamant et al. (1997), which leverages the lowest value of the first derivative of attenuated backscatter obtained by a lidar (B(z)) to detect the height of near-surface aerosol layers (H4) (Emeis, Schafer, & Munkel, 2008). This height is referred to as the Height of Gradient Minimum, denoted as $H4_{GM}$:

$$H4_{GM} = \min\left(\frac{\partial B(z)}{\partial z}\right) \quad (1)$$

Menut et al. (1999) introduced an alternative method known as the Inflection Point Method. It involves identifying the minimum of the second derivative of B(z) as an indicator of the Mixed Layer Height (MLH):

$$H4_{IPM} = \min\left(\frac{\partial^2 B(z)}{\partial z^2}\right) \tag{2}$$

This method tends to yield slightly lower values for H4 than the gradient method. According to Sicard et al., the MLH derived from radiosonde data using the Richardson number is closest to $H4_{IPM}$ (Emeis, Schafer, & Munkel, 2008). Another approach was pursued by Senff et al. (1999), where they sought the minimum value for the logarithm of the backscatter, referred to as the Height of Logarithmic Gradient Minimum, denoted as $H4_{LGM}$:

$$H4_{LGM} = \min\left(\frac{\partial B(z)}{\partial z}\right) \tag{3}$$

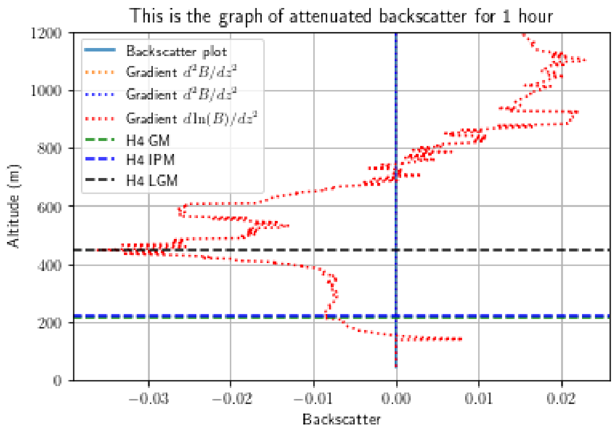

Figure 6. This plot shows the schematic line for three gradient methods to determine MLH. The IPM and GM values are really close to each other with 222m and 216m. The LGM is at 447m altitude.

The gradient method was further developed where equation 3 has been refined to enable the calculation up to n=5 lifted inversion (Emeis, Schafer, & Munkel, 2008). B(z) will denote the measured attenuated backscatter in height z average over time and Δh is the height averaging interval, then the gradient $\frac{\partial B}{\partial z}$ can be calculated as (Emeis, Schafer, & Munkel, 2008):

$$\left.\frac{\partial B}{\partial z}\right|_z = \frac{B\left(z+\frac{\Delta h}{2}\right)-B\left(z-\frac{\Delta h}{2}\right)}{\Delta h} \tag{4}$$

The value of Δh varies; when z is between 140 m and 500 m, Δh will be 80 m and when the layer is between 500 m and 2000m, the Δh is extended to 160m (Emeis, Schafer, & Munkel, 2008). For the second derivative of B(z), the gradient minimum is characterized by a change if sign from minus to plus. The second derivative of B(z) in height z is

$$\left.\frac{\partial^2 B}{\partial z^2}\right|_z = \frac{\left.\frac{\partial B}{\partial z}\right|_{z+\frac{\Delta h}{2}}-\left.\frac{\partial B}{\partial z}\right|_{z+\frac{\Delta h}{2}}}{\Delta h} \tag{5}$$

Thus, according to Emeis et al. (2008) the height of the aerosol layer ($H4_n$) will be equal to the height z if the all the conditions are met:

$$H4_n = z,\ if \begin{cases} \left.\frac{\partial^2 B}{\partial z^2}\right|_{z-1} \leq 0 \\ \left.\frac{\partial^2 B}{\partial z^2}\right|_{z} > 0 \\ B\left(z - \frac{\Delta h}{2}\right) \leq B_{min} \\ \left.\frac{\partial B}{\partial z}\right|_{z} \leq \frac{\partial B(z)}{\partial z}_{max} \end{cases} \tag{6}$$

The mix layer height from the doppler lidar backscatter is taken as the lowest height in $H4_n$.

4) Result and Discussion

4.1) Backscattering from Clouds and Aerosols

In this section, we will apply the threshold method to the raw data of attenuated backscatter to eliminate undesired data from the graphical representation. The backscatter data will exhibit a higher concentration in the lower regions of the atmosphere, as this is where the planetary boundary layer forms. Typically, the planetary boundary layer takes shape within 1000 meters above the surface. Through the analysis of attenuated backscatter, we will observe the formation of clouds and aerosols as we ascend in altitude.

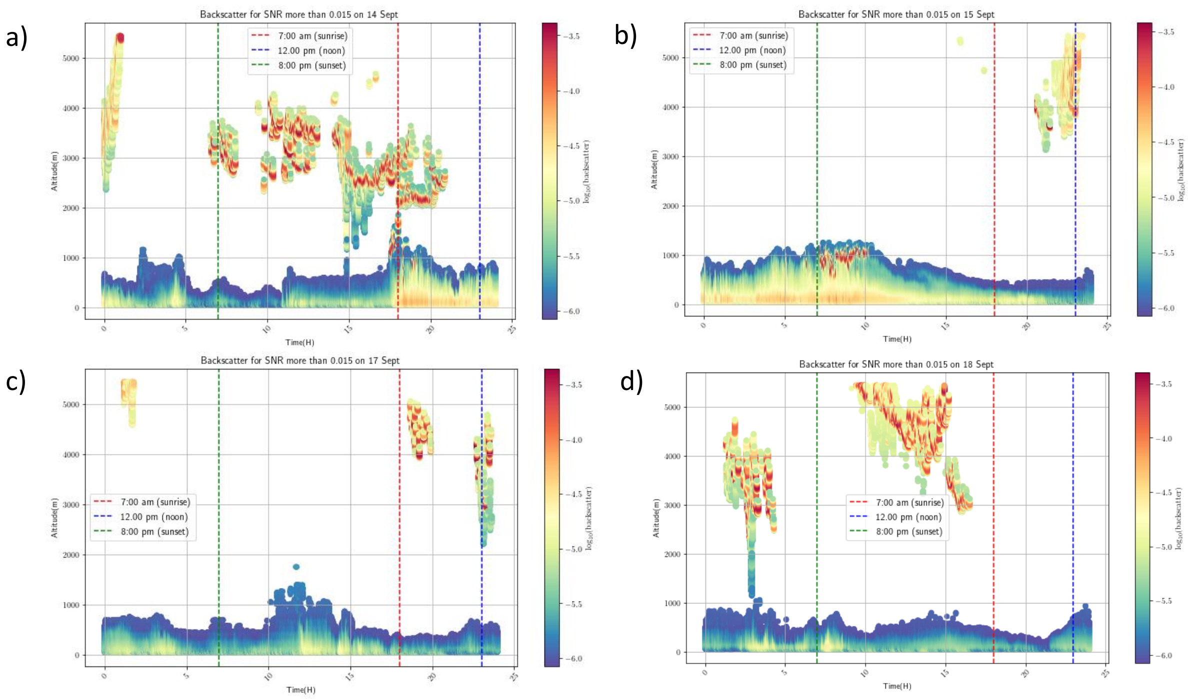

Figure 7. The $\log_{10}$ Backscatter plot where a threshold was applied to them. (a) and (b) are connected to each other as the sunrise of 15 September should be observed in (a) and the sunset on the same day was observed in figure (b). The same event applied to figure (c) and (d)

The attenuated backscatter observed in Figure 7 is noticeably more concentrated within the range of 1.5 km in altitude. The lower part of the troposphere is situated close to the surface layer, which is the primary source of aerosols in the atmosphere. Most of the aerosols at this site are suspected to be of natural origin, as it is located far from industrial areas. Natural aerosols, such as dust and maritime aerosols, are relatively large in size. Consequently, the Single Scattering Albedo (SSA) is higher for these types of particles, and they dominate when measured using remote sensing techniques (Dey & Tripathi, 2014). Comparing Figure 4 and Figure 7, we can roughly discern that the structure of the planetary boundary layer in the lower part of the atmosphere is similar to the PBL formation depicted in Figure 4. This suggests that the planetary boundary layer indeed exists within the altitude range of 1.5 km.

The attenuated backscatter data also allows us to observe the presence of clouds in the atmosphere, as evident in Figure 7. It's quite evident that the highest amount of cloud formation occurred on the night of September 14th. Liquid water clouds can be identified by a thin layer exhibiting very high backscatter at the cloud base (Illighworth, et al., 2019). Most of the clouds identified by the backscatter coefficient were situated above 2 km in altitude, and throughout the observation period, we only observed low-altitude clouds forming on September 15th. Interestingly, we were also able to observe the backscattering caused by precipitation falling from the clouds just below the cloud base. The clouds and rain appear in various shades of red, orange, and yellow, yielding results that are somewhat consistent with the work done by Illingworth et al. (2019) as depicted in Figure 8

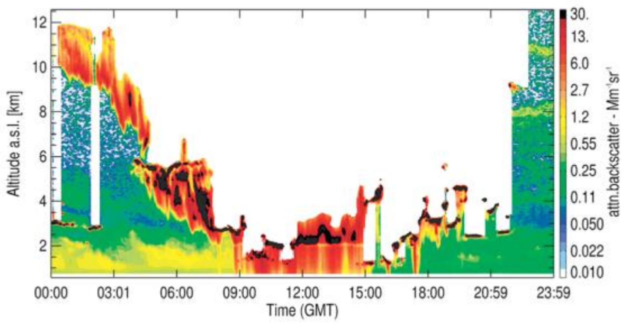

Figure 8. The 1064nm attenuated backscatter taken by a ceilometer where the and the rain appear in black, red and orange colours *(Illighworth, et al., 2019)*.

4.2) MLH Retrieval from Gradient Method

The filtered backscatter coefficient obtained through the threshold method was further analyzed to estimate the mixing layer height. The gradient method discussed in section 3.3 was applied to the backscatter data, and the results of this computation are presented in Figure 9.

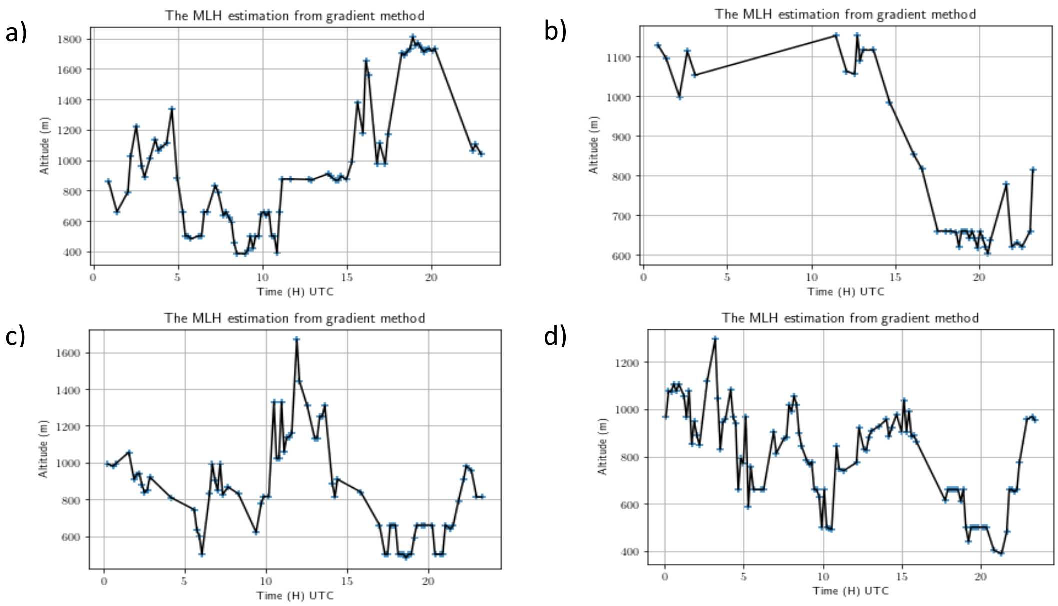

Figure 9. The plot shows the result obtain from the gradient method on estimating MLH. The '+' sign on the peak of the plot represent the peak of the MLH. Each (a), (b), (c) and (d) are the data from different day which is 14th, 15th, 17th and 18th of September.

From the MLH estimation results shown in Figure 9, it's evident that most of the MLH estimates using this method are approximately 1000 meters, especially on September 14th and 15th. The highest MLH estimate was on September 14th, reaching up to 1800 meters. This height is approximately 400 meters higher than the observed planetary boundary layer noted in the backscatter coefficient. In Figure 9 (b),(c) and (d), the MLH seems to decrease with mostly start at 15:00UTC.

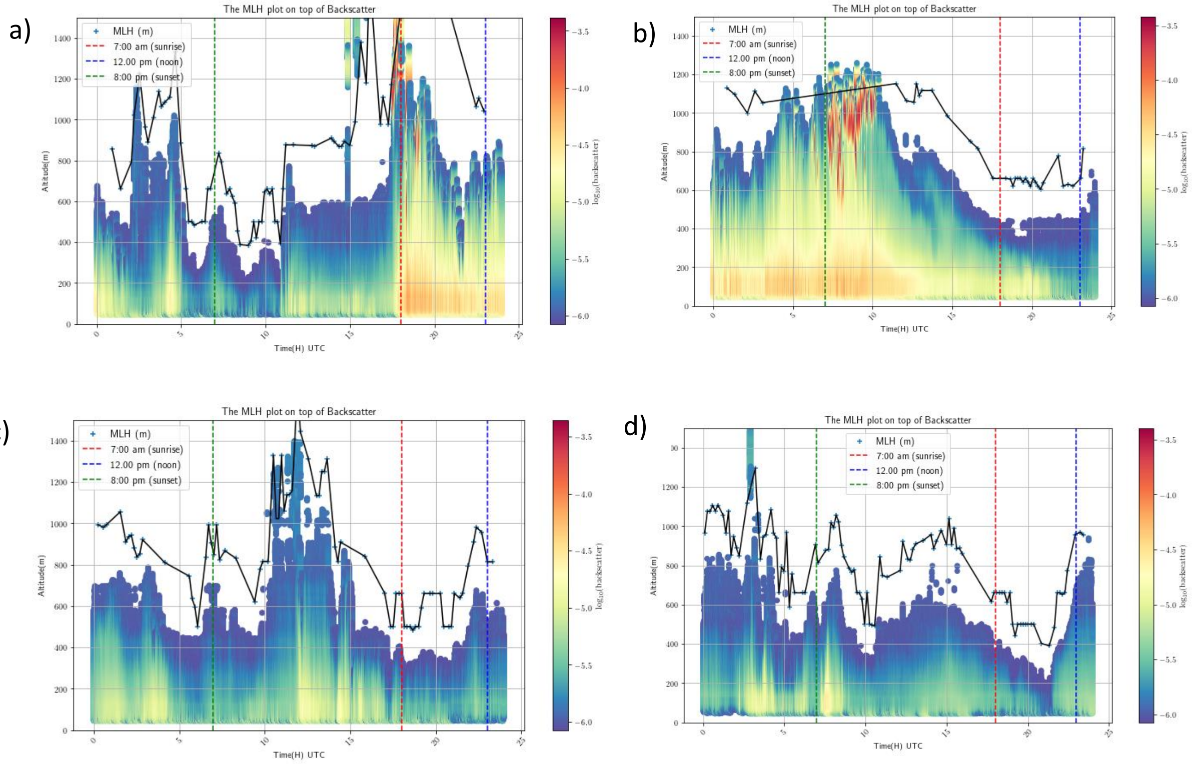

Figure 10. (a), (b), (c) and (d) are the comparison of the estimated MLH and the planetary boundary layer on the same chosen date which is 14, 15, 17 and 18 September.

Looking at Figure 10, it becomes clear that almost all the estimated mixing layer heights are well above the planetary boundary layer. This suggests that the estimations were far from our expected MLH value, based on the aerosol concentration within the PBL. Nevertheless, these estimations provide us with a rough idea of how the MLH changes with time. A substantial depth of MLH can be observed before sunset in Figure 10 (a), (b), and (d), which is around 05:00 UTC. During this period, the surface temperature is hotter than at other times, owing to the solar radiation received. In Figure 10 (c), it appears that the MLH layer is gradually expanding between 15:00 UTC and 22:00 UTC.

The results obtained for the estimation of the mixed layer height, as shown in Figure 10, are not reasonable because the height interval used was not suitable for the data. The initial height interval was based on the proposal by S. Emeis et al., using a Δh value of 80 meters between 140 meters and 500 meters and 160 meters between 500 meters and 2000 meters. The height interval may depend on the size of the PBL at the specific location. This method was repeated with different Δh values, specifically 30 meters and 60 meters between 60 meters to 420 meters and 420 meters to 1000 meters. The MLH estimated using the new height interval provides more reasonable results, as shown in Figure 11. The MLH estimations are more aligned with the boundary layer.

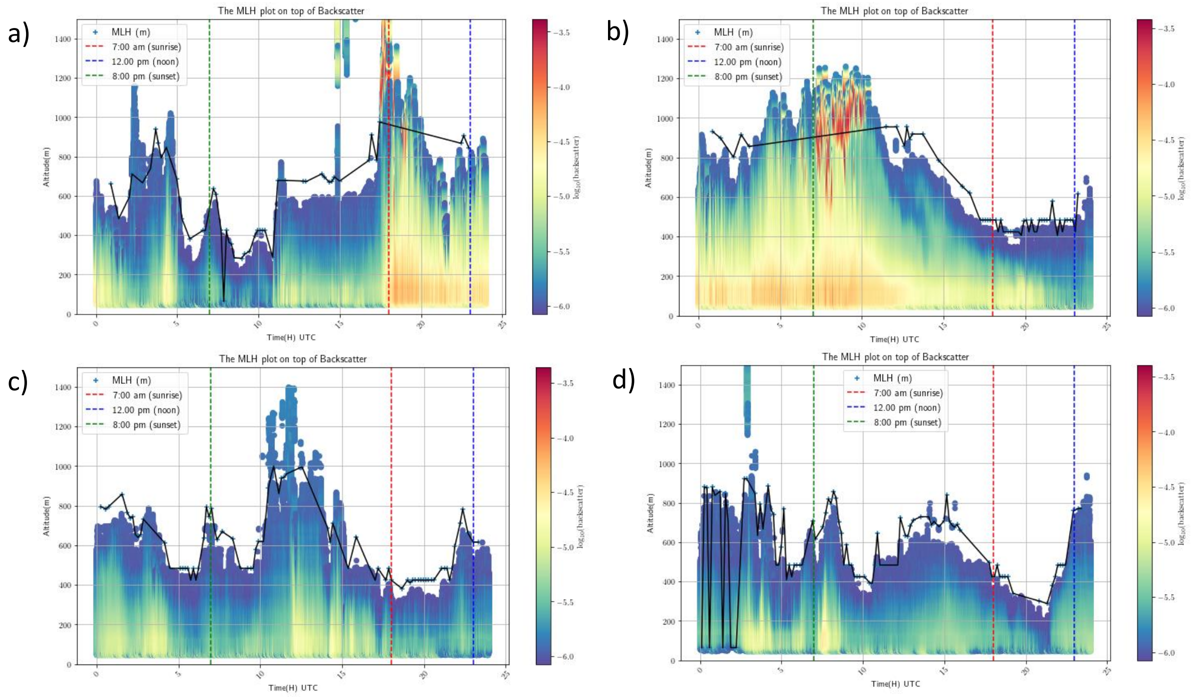

Figure 10. This is the MLH estimation result with height interval value of 30 m and 60 m.

4.3) Improvement on Estimating MLH

he results obtained were inconsistent, with periods where MLH estimates were missing, even when aerosol concentrations within the PBL were at their highest. To address this issue, we can enhance MLH estimation by employing multiple techniques simultaneously. S. Emeis et al. (2008) proposed more advanced methods for estimating the MLH, including the idealized backscatter method and the wavelet method. By examining the correlation between two or more methods, we can strive for a more accurate estimation and a conclusive result. Another potential method involves using vertical velocity data and applying a threshold value to the standard deviation of vertical velocity (Schween, Hirsiko, Löhnert, & Crewell, 2014). A similar approach was undertaken by Dewani et al. (2023) but with a different strategy.

Another limitation in this project is the restricted amount of backscatter coefficient data for aerosols, primarily due to the decreasing resolution of the Doppler lidar as altitude increases. To address this challenge, expanding the project by collecting data from additional instruments and extending the observation period can provide more data for MLH estimation. A ceilometer would be a valuable instrument to complement the Doppler lidar, as it can collect backscatter data up to 7.5 km(Dewani, Sakradzija, Schlemmer, Leinweber, & Scmidli, 2023).

5) Conclusion

In this research, we harnessed Doppler lidar vertical profile measurements spanning a one-week data collection period. We also incorporated attenuated backscatter data acquired through Doppler lidar to derive estimations for the mixing layer height (MLH). Furthermore, we conducted in-depth analyses of height variations during both daytime and nighttime. This study was conducted at a location owned by Tāwhaki, situated at Kaitorete Spit, where we employed the Halo Photonics Streamline XR Doppler lidar.

Two methods were employed for data analysis in this paper: the threshold method and the gradient or derivative method. The attenuated backscatter data from the Doppler lidar were initially filtered using a signal-to-noise ratio (SNR) threshold set at 0.015. Subsequently, the filtered data underwent analysis using the derivative method, with the aim of determining the altitude that met specific conditions, including the first and second derivative of backscatter concerning altitude, referred to as the height of the near-surface aerosol layer (H4_n). The MLH derived from this method corresponds to the lowest height of $H4_n$.

hrough these methods, we can conclude that employing a height interval (Δh) of 80 m and 160 m between two different altitude ranges resulted in the outcomes presented in Figures 9 and 10. The estimated MLH appears to be significantly higher than both the surface aerosol layer and the planetary boundary layer observed in the attenuated backscatter plots in Figure 10. The average MLH estimated for each day amounted to 996.98 meters, 812.29 meters, 850.01 meters, and 799.87 meters on the 14th, 15th, 17th, and 18th of September, respectively. However, these values seem somewhat unrealistic as they exceed the observed PBL height. We also applied the method with a different set of Δh values, specifically 20 meters and 40 meters between the altitudes of 60 meters to 420 meters and 420 meters to 1000 meters. The MLH estimation obtained from this approach appeared more reasonable, with the layer closer to the PBL. The average mixing layer height for these results was calculated as 591.88 meters, 574.55 meters, 603.46 meters, and 577.17 meters for the same dates.

Observations were made regarding the MLH estimation for each day, and we noticed that the MLH tended to expand after sunrise. This phenomenon is evident in Figures 11(c) and (d), where after sunrise in Figure 11(c), the estimated MLH gradually increased, reaching its peak in the evening, as depicted in Figure 11(d). However, we anticipated a decrease in MLH altitude during the nighttime, an event observed only once, as shown in Figure 11(a). Based on these observations, we can conclude that the MLH tends to expand during the daytime. However, the behaviour of the MLH at night remains uncertain, even though the MLH on September 14th, as indicated in Figure 11(a), appeared to decrease during the night and then began to increase as it approached sunrise.

Acknowledgments

I would like to express my sincere gratitude for the invaluable support provided by Professor Adrian McDonald and Grame Plank throughout the course of this project. I am also deeply appreciative of the dedication and contributions from my project collaborators, Idrees Hamid, Nicholas Plim, and Callum Miller. Additionally, I extend my thanks to Tāwhaki for generously permitting us to utilize their sites for this project.

References

Banakh, V. A., Smalikho, I. N., & Falits, A. V. (2021). Estimation of the height of the turbulent mixing layer from data of Doppler lidar measurements using conical scanning by a probe beam. *Atmos. Meas. Tech. , https://doi.org/10.5194/amt-14-1511-2021*, 1511-1524.

Beamesderfer, E. R., Biraud, S. C., Brunsell, N. A., Friedl, M. A., Helbig, M., Hollinger, D. Y., . . . Richardson, A. D. (2023). The role of surface energy fluxes in determining mixing layer heights. *Agriculture and forest meteorology, https://doi.org/10.1016/j.agrformet.2023.109687*, 1-17.

Dewani, N., Sakradzija, M., Schlemmer, L., Leinweber, R., & Scmidli, J. (2023). Dependency of vertical velocity variance on meteorological conditions in the convective boundary layer. *Atmos. Chem. Phys. https://doi.org/10.5194/acp-23-4045-2023*, 4045-4058.

Dey, S., & Tripathi, N. S. (2014). Remote science of atmospheric aerosol. In I. Colbeck, & M. Lazaridis, *Aerosol Science Technolgy and Applications* (pp. 120-126). United Kiingdom: John Wiley & Ons Ltd.

Emeis, S., Schafer, K., & Munkel, C. (2008). Surface-based remote sensing of the mixing-layer height - a review. *Meteorologische Zeitschrift, Vol. 17, DOI 10.1127/0941-2948/2008/0312*, 621-630.

Hayden, L. K., Anlauf, K. G., Hoff, R. M., Strapp, J. W., Bottenheim, J. W., Wiebe, H. A., . . . McKendry, I. G. (1997). *'93, J. Atmos. Environ*, 2089-2105.

Illighworth, A. J., Cimini, D., Haefele, A., Haefelin, M., Hervo, M., Kotthaus, S., . . . Potthast, R. (2019). How can existing ground-based profiling instruments improve European weather forecasts. *American Metereological Society*, 605-617.

Manninen, A. J. (2019). DEVELOPING METHODS FOR DOPPLER LIDAR TO INVESTIGATE ATMOSPHERIC BOUNDARY LAYER. *Institute for Atmospheric and Earth System Research / Physics, Faculty of Science, University of Helsinki, ISBN 978-952-7276-19-8, http://www.atm.helsinki.fi/FAAR/*, 1-42.

Ministry of Business, Inovation and Employment. (2022, 12 05). *Tāwhaki – a unique partnership focused on aerospace and environmental outcomes*. Retrieved from New Zealand research and partnership developtment, inovative partnership: https://www.mbie.govt.nz/science-and-technology/science-and-innovation/international-opportunities/new-zealand-r-d/innovative-partnerships/project-tawhaki/

Newsom, R., & Krishnamurthy, R. (2022). *Doppler Lidar (DL) Instrument Handbook.* Richland, Washington: U.S. Department of Energy, Atmospheric Radiation Measurement user facility.

Schween, J. H., Hirsiko, A., Löhnert, U., & Crewell, S. (2014). Mixing-layer height retrieval with ceilometer and Doppler lidar:. *Atmospheric Measurement Techniques, Inst. f. Geophysics and Meteorology, Univ. of Cologne, Cologne, Germany, www.atmos-meas-tech.net/7/3685/2014/doi:10.5194/amt-7-3685-2014*, 1-18.

Wang, X. Y., & Wang, K. C. (2014). Estimation of atmospheric mixing layer height from radiosonde data. *Atmos. Meas. Tech., www.atmos-meas-tech.net/7/1701/2014/doi:10.5194/amt-7-1701-2014*, 1701–1709.